

## DEP force

The dielectrophoretic force in its simplest implementation is the interaction of a nonuniform electric field with the dipole moment it induces in an object. The typical case is the induced dipole in a lossy dielectric spherical particle. The force in this case, where the particle is much smaller than the electric field nonuniformities, is given by

$$\mathbf{F} = 2\pi\varepsilon_m R^3 \operatorname{Re} \left[ \underline{CM}(\omega) \cdot \nabla \underline{\mathbf{E}}^2(\mathbf{r}, \omega) \right], \quad (1)$$

where  $\mathbf{F}$  refers to the dipole approximation to the DEP force,  $\varepsilon_m$  is the permittivity of the medium surrounding the sphere,  $R$  is the radius of the particle,  $\omega$  is the radian frequency of the applied field,  $\mathbf{r}$  refers to the spatial coordinate, and  $\underline{\mathbf{E}}$  is the complex applied electric field.  $\underline{CM}$  is the Clausius-Mossotti (CM) factor, which, for a lossy dielectric uniform sphere, such as a bead, is given by

$$\underline{CM} = \frac{\underline{\varepsilon}_2 - \underline{\varepsilon}_1}{\underline{\varepsilon}_2 + 2\underline{\varepsilon}_1}, \quad (2)$$

where  $\underline{\varepsilon}_1$  and  $\underline{\varepsilon}_2$  are the complex permittivities of the medium and the particle, respectively, and are each given by  $\underline{\varepsilon} = \varepsilon + \sigma/(j\omega)$ , where  $\varepsilon$  is the permittivity of the medium or particle,  $\sigma$  is the conductivity of the medium or particle, and  $j$  is  $\sqrt{-1}$ . Depending on the sign of the CM factor, the DEP force propels particles toward either the electric-field maxima (positive DEP, or pDEP) or minima (negative DEP, or nDEP).

Eq. 1 is the simplest approximation to the DEP force and does not account for higher-order components, where the field is sufficiently spatially nonuniform (in comparison to the size of the particle) to induce significant quadrupole and higher-order moments in the object. In addition, at field nulls the dipole moment is zero, because it is proportional to  $\underline{\mathbf{E}}$ , and therefore the dipole approximation to the DEP force (Eq. 1) will also be zero. In the mid-nineties, Washizu and Jones [1-3] developed a computationally accessible approach to calculating higher-order DEP forces. A compact tensor formulation of their result [1] is

$$\mathbf{F}^{(n)} = \frac{\overset{\cdot\cdot\cdot}{p}^{(n)} [\cdot]^n (\nabla)^n \underline{\mathbf{E}}}{n!}, \quad (3)$$

where  $n$  refers to the force order ( $n=1$  is the dipole,  $n=2$  is the quadrupole, etc.),  $\overset{\cdot\cdot\cdot}{p}^{(n)}$  is the multipolar induced-moment tensor, and  $[\cdot]^n$  and  $(\nabla)^n$  represent  $n$  dot products and gradient operations. Thus we see that the  $n$ -th force order is given by the interaction of the  $n$ -th-order multipolar moment with the  $n$ -th gradient of the electric field. This expression can be rewritten more explicitly for the time-averaged force in the  $i$ -th direction as

$$\begin{aligned} \langle F_i^{(1)} \rangle &= 2\pi\varepsilon_1 R^3 \operatorname{Re} \left[ \underline{CM}^{(1)} \underline{E}_m \frac{\partial}{\partial x_m} \underline{E}_i^* \right] \\ \langle F_i^{(2)} \rangle &= \frac{2}{3} \pi\varepsilon_1 R^5 \operatorname{Re} \left[ \underline{CM}^{(2)} \frac{\partial}{\partial x_m} \underline{E}_n \frac{\partial^2}{\partial x_n \partial x_m} \underline{E}_i^* \right], \\ &\vdots \end{aligned} \quad (4)$$

for the dipole ( $n=1$ ) and quadropole ( $n=2$ ) force orders [1]. The Einstein summation convention has been applied in Eq. 4. The multipolar CM factor for a uniform lossy dielectric sphere, such as a bead, is given by

$$\underline{CM}^{(n)} = \frac{\underline{\varepsilon}_2 - \underline{\varepsilon}_1}{n\underline{\varepsilon}_2 + (n+1)\underline{\varepsilon}_1} \quad (5)$$

The CM factor for cells, viruses, and bacteria is calculated using expressions from the literature [4]. More complex particle models could also be implemented.

To allow for an iterative force calculation algorithm, we need to catalog the multiple derivatives of the electric field, which are evaluated using nested loops. We do this with 6-dimensional matrices for the electric field and its derivatives arranged as  $E(x,y,z,p,q,r)$  where  $p$ ,  $q$ , and  $r$  correlate to the number of derivatives of the electric field taken in the  $x$ ,  $y$ , and  $z$  directions, respectively. Since Matlab only allows non-zero addressing into matrices, the following scheme is used

$$\begin{aligned} E(x,y,z,2,1,1) &= E_x \\ E(x,y,z,1,2,1) &= E_y \\ E(x,y,z,1,1,2) &= E_z \\ E(x,y,z,2,2,1) &= \frac{\partial E_x}{\partial y} = \frac{\partial E_y}{\partial x} \\ E(x,y,z,3,1,2) &= \frac{\partial^2 E_x}{\partial x \partial z} = \frac{\partial^2 E_z}{\partial x^2} \\ &\vdots \end{aligned} \quad (6)$$

While this labeling scheme is not memory-efficient, it simplifies the DEP force calculation algorithm, which is given by

$$\begin{aligned} \underline{F}_0^{(n)} &= \frac{2}{(n-1)!(2n-1)!!} \pi \varepsilon_1 R^{2n+1} \underline{CM}^{(n)} \\ \langle F_1^{(i)} \rangle, \langle F_2^{(i)} \rangle, \langle F_3^{(i)} \rangle &= 0 \\ \text{for } i &= 1 \text{ to } n \\ \langle F_1^{(i)} \rangle &= \langle F_1^{(i)} \rangle + \text{Re} \left[ \underline{F}_0^{(i)} \underline{E}(x,y,z,p,q,r) \underline{E}^*(x,y,z,p+1,q,r) \right] \\ \langle F_2^{(i)} \rangle &= \langle F_2^{(i)} \rangle + \text{Re} \left[ \underline{F}_0^{(i)} \underline{E}(x,y,z,p,q,r) \underline{E}^*(x,y,z,p,q+1,r) \right] \\ \langle F_3^{(i)} \rangle &= \langle F_3^{(i)} \rangle + \text{Re} \left[ \underline{F}_0^{(i)} \underline{E}(x,y,z,p,q,r) \underline{E}^*(x,y,z,p,q,r+1) \right] \\ \text{end;} \end{aligned} \quad (7)$$

where  $F_0^{(n)}$  is a constant calculated once and  $p$ ,  $q$ , and  $r$  are determined by a separate subroutine. In general, the electric fields and the CM factor are complex, so the real product is used to calculate the force.

### Other forces

In our modeling software we include four other forces – the hydrodynamic (HD) drag force, the HD lift force, the gravitational force, and the normal force from the rigid substrate top and bottom boundaries.

The HD drag force imposed on a stationary particle by a moving fluid is governed by low-Reynolds-number flow because of the small dimensions and low flow rates involved in these microsystems. When the particle sits close to the substrate, as in the nDEP square trap and pDEP trap, we are justified in using a shear flow approximation. The HD drag force is then similar to Stokes' drag on a sphere, with a correction for the effects of the wall [5]:

$$F_{drag} = 6\pi\mu R\dot{\gamma}F_{drag}^*z = 6\pi\mu R\left(6Q/wh^2\right)F_{drag}^*z \quad (8)$$

where  $\mu$  is the viscosity of the liquid,  $F_{drag}^*$  is a nondimensional factor incorporating the wall effects,  $z$  is the distance from the particle center to the substrate, and  $\dot{\gamma}$  is the shear rate at the wall in a parallel plate flow chamber, where  $Q$  is the flow rate,  $w$  is the chamber width, and  $h$  is the chamber height [6]. Li *et al.* showed that this shear flow approximation is valid even when the particle diameter occupies a significant fraction of the chamber height [7].

When the particle is not near the substrate, as in the nDEP octopole traps, we use a parabolic Poiseuille flow profile. The HD drag force is then [8]:

$$F_{drag} = 6\pi\mu R V_c F(z) = 6\pi\mu R(1.5Q/wh)F(z) \quad (9)$$

where  $V_c$  is the centerline velocity in the flow chamber and  $F(z)$  is a nondimensional factor incorporating the height of the particle in the chamber. Other analytical or non-analytical flow profiles can also be implemented. The applied flow, and therefore the HD drag force, is in the  $+x$  direction.

The magnitude of the gravitational force is given by

$$F_{grav} = -\frac{4}{3}\pi R^3(\rho_p - \rho_m)g \quad (10)$$

where  $\rho_m$  and  $\rho_p$  refer to the densities of the medium and the particle, respectively, and  $g$  is the gravitational acceleration constant. In our case, the particles are more dense than the medium and thus have a net downward force in the  $-z$  direction.

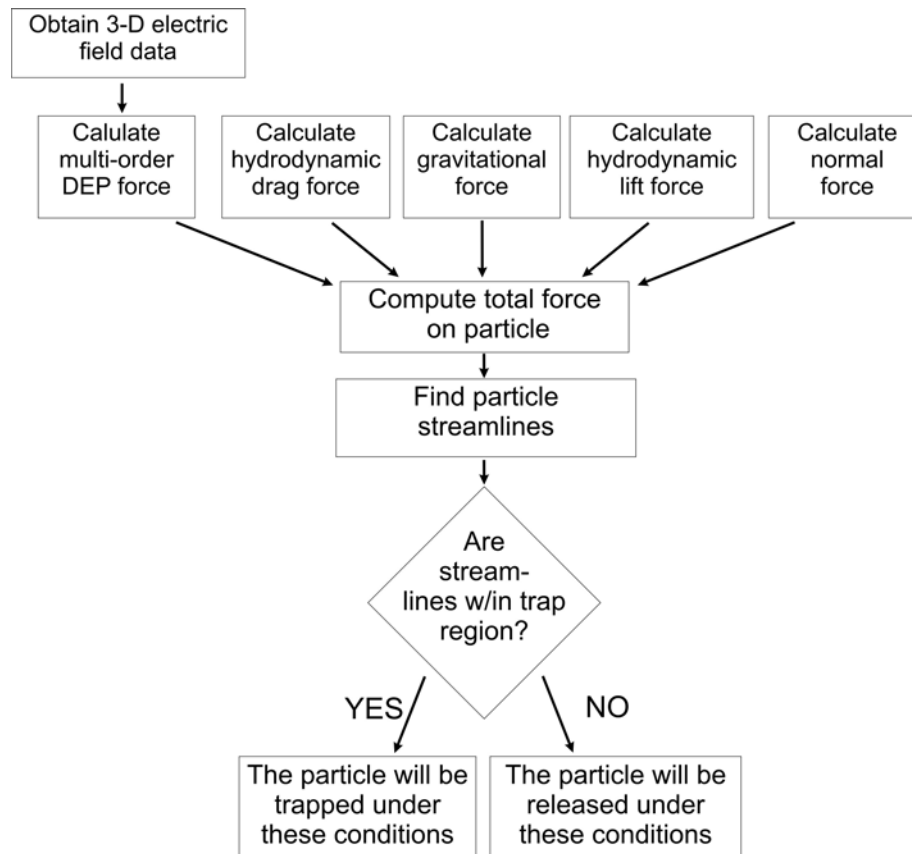
The HD lift force is caused by low-Reynolds-number viscous flow over an object near a solid plane, which tries to levitate the particle in the  $+z$  direction. For a stationary sphere in contact with the plane, the lift force becomes [9, 10]:

$$F_{lift} = 9.22\dot{\gamma}^2\rho_m R^4 = 9.22(36Q^2/w^2h^4)\rho_m R^4 \quad (11)$$

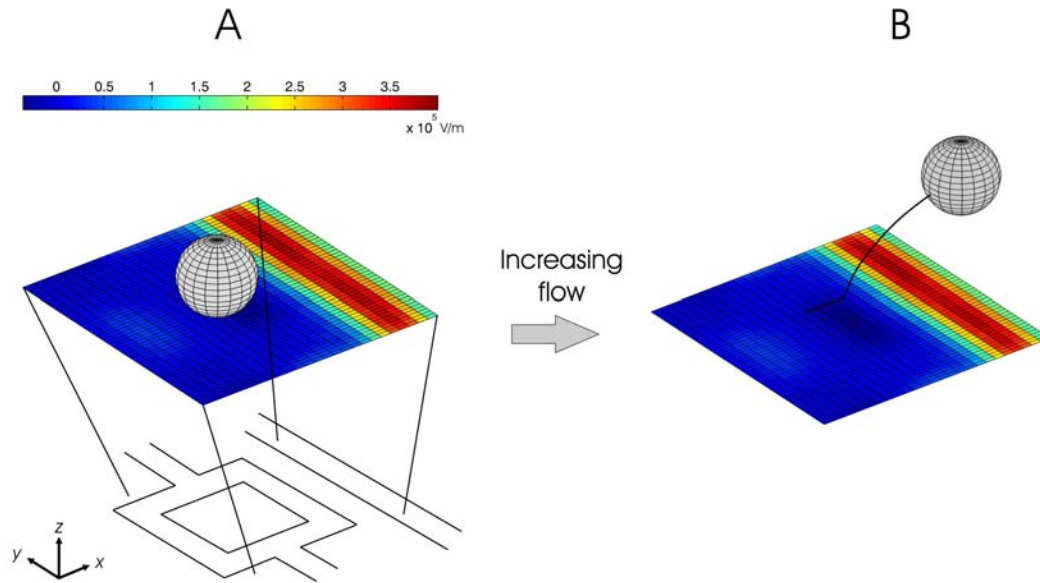
At lower flow rates, the lift force was found to be negligible compared to the  $z$ -directed DEP force and gravity. However, since the lift is proportional to  $Q^2$  and  $R^4$ , the lift force could become significant for higher flow rates and larger bead diameters. This was the case for the pDEP points-and-lid geometry, which had higher maximum flow rates.

Our final force is the implementation of a normal force in the  $-z$  and  $+z$  direction, produced by the top and bottom substrates. We implement this force using an algorithm that automatically adjusts the  $z$ -directed total force on the particle so that it is zero when the particle contacts the top or bottom surface.

## Supplemental Figures



**Supplemental Figure 1:** Overview of the modeling software, showing the major steps. From user-provided electric field data and other experimental parameters, the forces on the particle (DEP, HD drag, gravitational, HD lift, and normal) are computed everywhere in space. The total force on the particle is used to generate streamlines that determine if the particle is stably held in the trap.



**Supplemental Figure 2:** Particle streamlines for a 14- $\mu\text{m}$  cell when (A) the cell is stably held in the trap and (B) the flow exceeds the maximum flow rate and the cell is pushed out of the trap. The color bar shows the x-directed electric field intensity (in  $\text{V/m}$ ) for a  $5V_p$  applied signal.

## References

1. Jones, T.B. and M. Washizu, *Multipolar dielectrophoretic and electrorotation theory*. Journal of Electrostatics, 1996. **37**(1-2): p. 121-134.
2. Washizu, M. and T.B. Jones, *Multipolar Dielectrophoretic Force Calculation*. Journal of Electrostatics, 1994. **33**(2): p. 187-198.
3. Washizu, M. and T.B. Jones, *Generalized multipolar dielectrophoretic force and electrorotational torque calculation*. Journal of Electrostatics, 1996. **38**(3): p. 199-211.
4. Jones, T.B., *Electromechanics of Particles*. 1995: Cambridge University Press. 285.
5. Goldman, A., R. Cox, and H. Brenner, *Slow viscous motion of a sphere parallel to a plane wall - II Couette flow*. Chemical Engineering Science, 1967. **22**: p. 653-660.
6. Deen, W.M., *Analysis of Transport Phenomena*. 1998, New York: Oxford University Press. 624.
7. Li, H.B., Y.N. Zheng, D. Akin, and R. Bashir, *Characterization and modeling of a microfluidic dielectrophoresis filter for biological species*. Journal of Microelectromechanical Systems, 2005. **14**(1): p. 103-112.
8. Ganatos, P., R. Pfeffer, and S. Weinbaum, *A Strong Interaction Theory for the Creeping Motion of a Sphere between Plane Parallel Boundaries .2. Parallel Motion*. Journal of Fluid Mechanics, 1980. **99**(AUG): p. 755-783.
9. Leighton, D. and A. Acrivos, *The lift on a small sphere touching a plane in the presence of a simple shear flow*. Journal of Applied Mathematics and Physics, 1985. **36**: p. 174-178.
10. Cherukat, P. and J.B. McLaughlin, *The Inertial Lift on a Rigid Sphere in a Linear Shear-Flow Field near a Flat Wall*. Journal of Fluid Mechanics, 1994. **263**: p. 1-18.